scientific reports

Check for updates

OPEN

Enhanced alleviation of the selenite-grafted soluble and nondigestive Chinese Yam polysaccharides on nonylphenol-induced cytotoxicity and barrier damage in intestinal epithelial cells

Zhen-Xing Wang[1,2,3], Li-Li Zhang[2] & Xin-Huai Zhao[1,2]✉

This study explored the in vitro alleviation of the soluble and non-digestible Chinese yam polysaccharides (YP) with covalent selenite-grafting on the nonylphenol-induced cytotoxicity and barrier damage in rat intestinal epithelial (IEC-6) cells. Two grafted products YPSe-I and particularly YPSe-II possessed much higher Se contents than YP (0.803 and 1.486 *versus* 0.037 g/kg), could alleviate the cytotoxicity of nonylphenol by causing higher cell viability but lower lactate dehydrogenase release and ROS production, and were capable of repairing the induced barrier damage through increasing transepithelial electrical resistance, reducing paracellular permeability, promoting the production and distribution of cytoskeleton F-actin, and up-regulating the expression levels of three tight junction proteins namely zonula occludens-1, occludin, and claudin-1. Meanwhile, the expression levels of two proteins namely p-p38 and p-JNK in the cells, which are crucial to the activation of the MAPK signaling pathway, were up-regulated by nonylphenol but down-regulated by YPSe-I and YPSe-II. The results consistently confirmed that YP and YPSe-II exhibited the respective lowest and highest activities in the cells to alleviate the nonylphenol-induced cytotoxicity and barrier damage, declaring that both YP selenization and higher selenite-grafting extent were the critical factors controlling the measured activities of YPSe-I and YPSe-II. Collectively, this selenite-grafting of YP endowed the selenized products with higher activity in the cells to reduce nonylphenol-induced cytotoxicity, especially to alleviate the induced barrier damage by inactivating the MAPK signaling pathway.

Keywords Yam polysaccharides, Selenization, Nonylphenol, Intestinal barrier, Tight junction protein, MAPK signaling pathway

Nonylphenol polyoxyethylene ethers (NPEs) are widely used in the industrial production of textiles, paper, and others. When NPEs are degraded in nature, an organic substance specifically nonylphenol is released from NPEs and causes pollution to the environment[1] Nonylphenol exhibits relatively high stability, making it difficult to remove completely through conventional treatment methods such as adsorption or advanced oxidation. It can persist in water, soil or sediments for a long-time period,[2] and is thus regarded as one of the persistent organic pollutants. Nonylphenol, being a lipophilic substance, is capable of infiltrating organisms *via* respiratory processes or alternative ways. As a consequence, it accumulates in components like adipose tissue[3] When nonylphenol enters foodstuffs through the food chain, it will pose a potential harmful impact on the body. For example, when tomato and lettuce had root exposure to the nonylphenol-polluted irrigation water, the measured nonylphenol contents in tomato fruits and lettuce leaves were up to 46.1 and 144.1 μg/kg[4]. It has been estimated in a literature that the nonylphenol concentration in foods ranges from 0.1 to 1000 μg/kg[5]. Unfortunately, nonylphenol has been identified as an endocrine disruptor in the body. Long-term exposure of the body to the

[1]School of Biology and Food Engineering, Guangdong University of Petrochemical Technology, Maoming 525000, China. [2]College of Food Science, Northeast Agricultural University, Harbin 150030, China. [3]College of Food Engineering, Harbin University of Commerce, Harbin 150076, China. ✉email: zhaoxh@neau.edu.cn

nonylphenol-rich foods may result in disorders of the endocrine system. For example, nonylphenol can affect the level of sex hormones, which may trigger a series of health problems including abnormal development of the reproductive system and decreased fertility[6] Additionally, nonylphenol is associated with an increased incidence of certain cancers. By interfering with intracellular signal transduction pathways, nonylphenol affects both cell proliferation and differentiation, and thus elevates the risk of cancer[7] Overall, the scientific community has paid special attention to the adverse effect of nonylphenol on the body.

Beyond its primary roles in nutrient absorption and digestion, the intestine is recognized as critical to human health, due to its additional functions including defending against the intraluminal pathogens[8] The intestine must maintain selective permeability to ensure the optimal absorption of various nutrients, and also performs barrier function to prevent harmful microorganisms or toxins and other substances from entering the body through the intestine. Thus, the maintenance of intestinal barrier integrity is essential for preserving systemic homeostasis. Composed of a monolayer of interconnected epithelial cells, the intestinal epithelium constitutes the body's largest interface with the external environment[9] Specialized junctional complexes, including tight junctions (TJ), adherent junctions, and desmosomes, collectively establish a regulated permeability barrier at the apex of intestinal epithelial cells (IEC)[10] This barrier permits the selective passage of nutrients and water, but effectively excludes pathogenic bacteria, viruses and antigenic substances. However, exposure to xenobiotics (like nonylphenol and indomethacin) has been shown to injure intestinal barrier integrity. Fortunately, certain dietary components have demonstrated protective effect against toxin-induced barrier dysfunction. For instance, the results from our research group showed that the oligochitosan-glycated caseinate digest could mitigate the acrylamide-induced barrier impairment in IEC-6 cells,[11] while two polyphenolic compounds namely galangin and kaempferol also might attenuate the indomethacin-induced cytotoxicity and barrier disruption in IEC-6 cells[12] In addition, other researcher had reported that *Gracilaria lemaneiformis* polysaccharides could alleviate the intestinal damage caused by colitis in mice, through improving intestinal flora[13].

Se is one of the essential trace elements in human physiology. Since Se can not be endogenously synthesized in the body, adequate Se must be obtained through dietary sources including the Se-containing foods or specially Se-containing drugs. Inorganic Se has reduced bioavailability and potential toxicity upon accumulation. In contrary, organic Se demonstrates enhanced bioavailability and reduced toxicity. Inorganic Se can be converted into organic Se through appropriate chemical or biological modification. For example, the selenite groups could be covalently bound to polysaccharide and protein molecules by chemical modification,[1415] or Se could be incorporated into yeast through a cultivation in Se-enriched media to yield the Se-rich yeast[16] Thus, food macromolecules like polysaccharides and proteins are selenized (or Se-grafted) covalently to enhance their Se contents and particularly bioactivity. For example, the antioxidant activity of ovalbumin was enhanced after a chemical selenization,[15] while the Se-containing peptides derived from Se-rich protein hydrolysates had improved immunomodulatory effect in the LPS-induced RAW264.7 cells[17] Furthermore, *Pleurotus eryngii* polysaccharides with chemical selenization also showed higher immune activity than the unselenized ones[18].

The soluble, nondigestible, and nonstarch yam components, namely yam polysaccharides (YP), exhibit multiple bioactive properties. A study revealed that YP was able to reduce blood lipids by regulating the composition and abundance of intestinal flora, influencing the types of intestinal metabolites, and improving the deposition of liver and perirenal fat[19] Furthermore, it was found that YP enhanced the intestinal abundance of *Megasphaera* and *Bifidobacterium*, increased short-chain fatty acid production, and thereby exhibited anti-inflammatory effect in the LPS-stimulated Caco-2 and Raw264.7 cells[20] However, the question of whether chemical selenization of YP by grafting the $HSeO_3$ group serves to enhance or reduce its protective capacity against the nonylpheno-induced cytotoxicity and barrier loss within intestinal epithelial cells remains an open and undetermined issue. Thus, an investigation using cell model deserves our consideration.

In this study, fresh Chinese yam tubers were used to prepare the targeted YP. Two selenite-grafted YP products (namely YPSe-I and YPSe-II) with varying Se contents or selenite-grafting extents were prepared using nitric acid and sodium selenite, which caused a covalent selenite-grafting of YP. YP, YPSe-I, and YPSe-II were applied to rat intestinal epithelial (i.e., IEC-6) cells with or without nonylphenol damage, while the cells were detected for these indices related to cell toxicity and barrier dysfunction. The expression of three TJ proteins including zonula occludens-1 (ZO-1), occludin, and claudin-1, or that of p-p38 and p-JNK involved in the MAPK signaling pathway, were also detected at both mRNA and protein levels. The aim of this study was to reveal whether the conducted covalent selenite-grafting of YP could cause higher activity to alleviate the nonylphenol-induced cytotoxicity and barrier disruption in the intestine.

Materials and methods

Chemicals and reagents

The fresh yam tubers were commercially purchased from the local market in Harbin (Heilongjiang Province, China). Nonylphenol (CAS No. 84852-15-3), 4 kDa fluorescein isothiocyanate-dextran (FD-4), 3-(4,5-dimethyl-2-thiazolyl)-2,5-diphenyl tetrazolium bromide (MTT), fluorescein sodium (FS-Na), and Dulbecco's modified Eagle's medium (DMEM) were purchased from Sigma-Aldrich Co. (St. Louis, MO, USA). Phosphate-buffered saline (PBS) and dimethyl sulfoxide (DMSO) were purchased from Solarbio Science and Technology Co., Ltd. (Beijing, China). Alkaline protease was purchased from Beijing Aoboxing Biotechnologies, Inc. (Beijing, China), while Actin-Tracker Red-Rhodamine, bicinchoninic acid (BCA), phenylmethanesulfonylfluoride (PMSF), and radio-immunoprecipitation assay (RIPA) kits were obtained from Beyotime Institute of Biotechnology (Shanghai, China). Other chemicals used in this study were of analytical grade. The water used was ultrapure water generated from a Milli-Q Plus (Milipore Corporation, New York, NY, USA).

RNAprep Pure Cell Bacteria Kit was purchased from Tiangen Biotech Co., Ltd. (Beijing, China), and the NovoScript® Two-Step RT-PCR Kit and SYBR qPCR SuperMix Plus were purchased from Novoprotein Biotech Co., Ltd. (Suzhou, China). Primary antibodies (GAPDH Bioss bs-10900R, ZO-1 Bioss bs-1329R) and goat anti-

rabbit secondary antibody were all purchased from Bioss Biotechnology Co., Ltd. (Beijing, China). Claudin-1 (28674-1-AP) and occludin (13409-1-AP) were purchased from Proteintech Group Inc. (Wuhan, China), while p-p38 (#4511) and p-JNK (#4668) were the products of Cell Signaling Technology (Danvers, MA, USA).

Cell line and cell culture

The rat intestinal epithelial cell line (IEC-6 cells) was obtained from the American Type Culture Collection (Rockville, MD, USA). The cells were cultured in the required DMEM containing fetal bovine serum (10%), sodium pyruvate (1%), bovine insulin (0.1% units/mL), and penicillin-streptomycin (100 U/mL), and maintained at 37 °C in a humidified environment containing 5% CO_2.

Preparation and covalent selenite-grafting of YP

As previously described[21], YP was separated from fresh yam tubers and freeze-dried after ethanol precipitation. Afterwards, YP of 1 g was selenite-grafted using 1% (v/v) HNO_3 and 50 or 100 mg Na_2SeO_3.[22] After the specified selenization reaction, ethanol precipitation, ethanol washing and freeze-drying, two covalent selenite-grafted products namely YPSe-I and YPSe-II were obtained and used in subsequent experiments together with YP. Moreover, Se contents of YP, YPSe-I, and YPSe-II were analyzed using a inductively coupled plasma-mass spectrometer (Agilent Technologies, Santa Clara, CA, USA).

Assaying of nonylphenol cytotoxicity

IEC-6 cells were plated on 96-well plates at a density of 2×10^3 cells/well, cultured until confluence for 24 h, and then transferred to the serum-free medium for 12 h. For nonylphenol cytotoxicity assessment, the cells were treated with nonylphenol at 20, 40, 60, 80, 100, 120, 140, and 160 μg/mL, and incubated for 24 h. After discarding the supernatant, 100 μL of MTT (0.5 μg/mL) was added to each well, and the cells were further incubated at 37 °C for 4 h. After removing the supernatant, 100 μL of DMSO was added to each well. The cells were gently shaken and incubated again at 37 °C for 2 h. The optical density of each well at 490 nm was measured using a microplate reader (Bio-Rad Laboratories, Hercules, CA, USA). The viability value was calculated as previously described,[23] while the cells treated with normal medium only were used as a control with a designated viability value of 100%. The IC_{50} value of nonylphenol in IEC-6 cells was then calculated as previously described[24].

To detect the effect of YP, YPSe-I, and YPSe-II on IEC-6 cells, the cells (2×10^3 cells per well) were seeded on 96-well plates, cultured until confluence for 24 h, serum-starved for 12 h, and incubated with fresh medium containing or lacking YP, YPSe-I, and YPSe-II at various final concentrations (5, 10, 20, and 40 μg/mL). The cells were incubated for respective 12 and 24 h, and then incubated with 120 μg/mL nonylphenol for 24 h, followed by the addition of 100 μL of 0.5 μg/mL MTT solution and the incubation of 4 h at 37 °C. After then, the optical density of each well at 490 nm was measured as above. The viability value was thus estimated and reported as a percentage of the control cells (without nonylphenol injury but designated with viability value of 100%).

Determination of lactate dehydrogenase release

For the determination of lactate dehydrogenase (LDH) release, IEC-6 cells (2×10^3 cells/well) were seeded in 96-well plates, synchronized in serum-free medium for 12 h, and treated with or without YP, YPSe-I, and YPSe-II (5, 10, 20, and 40 μg/mL) for 12 and 24 h, respectively. The cells were then exposed to 120 μg/mL nonylphenol for 24 h and centrifuged at 190×*g* for 5 min. The supernatants were collected and analyzed for LDH activity using a commercial assay kit according to the manufacturer's protocol. The cells treated with normal medium only were used as a control with designated LDH release value of 100%[11].

Determination of transepithelial electrical resistance and paracellular permeability

For the assessment of epithelial barrier function, IEC-6 cells were seeded on Transwell inserts (12 mm diameter, 0.4 μm pore size, polyester membranes, Corning) at a density of 2×10^5 cells/cm² in 0.5 mL medium, while 1.5 mL culture medium was added to the basolateral side. The medium was replaced every other day. Transepithelial electrical resistance (TEER) value was measured using a Millicell-ERS2 volt-ohmmeter (Millipore, Bedford, MA, USA) till TEER value reached to 50 Ω cm². To evaluate the barrier protection, confluent monolayers were pretreated with YP, YPSe-I, and YPSe-II (5, 10, 20, and 40 μg/mL) for 12–24 h, followed by the nonylphenol exposure (120 μg/mL) of 24 h. TEER value was measured before and after these treatments and calculated as previously described[25].

Following the established Transwell culture protocol, IEC-6 monolayers were pretreated with YP, YPSe-I, and YPSe-II (5, 10, 20, and 40 μg/mL) for 12–48 h prior to 24 h exposure of 120 μg/mL nonylphenol. To assess barrier integrity, either fluorescein isothiocyanate FD-4 (0.5 mg/mL) or FS-Na (0.08 mg/mL) was introduced to the apical compartment. After an incubation of 24 h at 37 °C, fluorescence intensity in basolateral medium was quantified using a fluorescent microplate reader (Infinite M200 pro, TECAN, Männedorf, Switzerland) with excitation/emission wavelengths of 490/520 nm. Paracellular permeability was thus calculated as the percentage of fluorescence intensity relative to the untreated control (designed as 100% paracellular permeability), using the established methodologies[1226].

Determination of intracellular reactive oxygen species

IEC-6 cells were seeded into 6-well plates at a density of 4×10^5 cells per well, cultured for 24 h to allow their adhere, and subsequently maintained in serum-free medium for 12 h. Following medium removal, the cells were cultured with 2 mL of medium or YP, YPSe-I, and YPSe-II at 5, 10, 20, and 40 μg/mL for 12–24 h. Subsequently, nonylphenol at 120 μg/mL was introduced, and the cells were further incubated for 24 h. One milliliter of reactive oxygen species (ROS) fluorescent probe (2',7'-dichlorodihydrofluorescein diacetate, DCFH-DA, 5 μmol/L) was

used for cell staining in the dark for 20 min. Following the DCFH-DA staining, the cells were transferred into 96-well plates. Fluorescence intensity was measured using the fluorescent microplate reader at excitation/emission wavelengths of 488/525 nm. The relative ROS level of the treated cells were calculated as a percentage value of that of control cells (designed with relative ROS level of 100%)[27].

Fluorescence staining labeling of cytoskeletal F-actin

The distribution of F-actin among the cells was visualized using the rhodamine-labeled phalloidin, as previously described[28] Specifically, IEC-6 cells (2×10^5/well) were seeded into 12-well plates and allowed to adhere completely before the treatment with YP, YPSe-I, and YPSe-II at 40 μg/mL for 12 and 24 h, respectively, followed by the exposure of 120 μg/mL nonylphenol for 24 h. Finally, F-actin distribution was assessed and imaged using a fluorescence microscopy (OLYMPUS IX71, OLYMPUS Corporation, Tokyo, Japan).

Quantitative real-time qPCR analysis

The mRNA expression levels of ZO-1, claudin-1, occludin, p-p38, and p-JNK were quantified using quantitative real-time qPCR. Following the treatment with YP, YPSe-I, and YPSe-II at 40 μg/mL for 24 h, the cells were exposed to nonylphenol (120 μg/mL) for 24 h. According to the kit instruction, total RNA was extracted using the RNAprep Pure Cell/Bacteriology Kit (Life Technologies Corporation, Carlsbad, CA) and then reverse-transcribed into cDNA using the NovoScript® SYBR qPCR SuperMix Plus and Biosystems StepOnePlus real-time PCR system. The resulting cDNA was used as template DNA, while PCR assays were performed using the specific primers given in Table 1. Glyceraldehyde 3-phosphate dehydrogenase (GAPDH) was used as a control, and relative expression levels of each targeted gene were analyzed using the $2^{-\Delta\Delta Ct}$ method as previously described[29].

Western-blot assay

The protein expression levels of ZO-1, claudin-1, occludin, p-p38, and p-JNK were analyzed by western-blot assay. First, the cells were treated with or without YP, YPSe-I, and YPSe-II at 40 μg/mL for 24 h and then exposed to 120 μg/mL nonylphenol for 24 h. Afterwards, the treated cells were collected and lysed for 30 min with 1 mmol/L PMSF and RIPA lysis buffer on ice for total protein extraction. After centrifuging at 14,000×*g* for 5 min, the supernatants were collected, and protein concentrations were determined using BSA protein assay kit. An equal amount of protein (15 μg) from each sample was separated by 12% SDS-PAGE and then transferred to nitrocellulose membranes. The targeted protein bands were blocked with 5% skim milk for 2 h at 37 °C, incubated with primary antibodies (1:1000 dilution) at 4 °C for 12 h, and then incubated with the secondary antibody (1:5000 dilution) for 2 h at 37 °C. Ultimately, the bands were visualized with an Amersham Imager 600 (General Electric Company, Boston, MA, USA), while quantitative analysis was conducted using Image J software version 1.50b (National Institutes of Health, Bethesda, MD, USA). As usual, protein expression levels were normalized to GADPH[30].

Statistical analysis

All values were acquired after three independent experiments or assays, and were reported as mean values or mean values ± standard deviations. Significant differences ($p < 0.05$) between the means of multiple groups were determined by one-way analysis of variance (ANOVA) with Duncan's multiple range tests in SPSS 22.0 software (SPSS Inc., Chicago, IL, USA).

The ethics approval

This is an in vitro project on rat intestinal epithelial cells and has no ethical code.

Gene	Species	Primer (5' – 3')	
ZO-1	Rat	FORWARD	CCACCTCGCACGTATCACAAGC
		REVERSE	GGCAATGACACTCCTTCGTCTCTG
Occludin	Rat	FORWARD	CCTCCTTACAGGCCGGATGA
		REVERSE	AGCATTGGTCGAACGTGCAT
Claudin-1	Rat	FORWARD	GTTTCATCCTGGCTTCGCTG
		REVERSE	AGCAGTCACGATGTTGTCCC
p-p38	Rat	FORWARD	CCTCAGCTCAGCGAGAGAAT
		REVERSE	GGCACATTTAAGCTGGGCAC
p-JNK	Rat	FORWARD	GCGACTGGAATGAGAACACAG
		REVERSE	CTGGAACTTACTGAAGCCACC
GAPDH	Rat	FORWARD	CCCTCTGGAAAGCTGTGG
		REVERSE	GCTTCACCACCTTCTTGATGT

Table 1. The sequences of the primers used in RT-qPCR assays.

Results

Nonylphenol cytotoxicity in IEC-6 cells

To evaluate the impact of the targeted polysaccharide sample on intestinal barrier function under nonylphenol exposure, it was essential to determine potential cytotoxic effect of nonylphenol on IEC-6 cells using the classic MTT method (Fig. 1). Cell treatment with nonylphenol at 20–160 μg/mL for 24 h caused a reduction in viability value (28.8–98.8%), regarding the control cells (viability value 100%). Higher nonylphenol dose consistently led to much reduction in viability value. That is, nonylphenol dose-dependently exerted cytotoxicity on the cells. Based these obtained results, it was estimated that the IC_{50} value of nonylphenol in IEC-6 cells was near 129 μmol/L. Additionally, nonylphenol dose of 120 μg/mL caused viability value of 65.7%, suggesting this dose was efficient to induce cytotoxic effect in the cells. Thus, nonylphenol dose of 120 μg/mL was selected in the later experiments of this study to injure the cells.

Inhibitory effect of prepared polysaccharide samples on nonylphenol cytotoxicity

In this research, YP underwent chemical selenization in the presence of Na_2SeO_3 and HNO_3. Chemically, this process introduced functional groups as $HSeO_3$ to the saccharide units in the polysaccharide molecules. During the preparation of YPSe-I and YPSe-II, free Se (i.e. the unreacted selenious acid) was removed through ethanol precipitation and subsequent ethanol washes, because of different solubility of polysaccharides (ethanol-insoluble) and selenious acid (ethanol-soluble). The present analysis results showed that YPSe-I and YPSe-II had respective Se contents of 0.803 and 1.486 g/kg, which were much higher than that of YP (0.037 g/kg only). Due to its higher Se content, YPSe-II received greater covalent selenization and thus had higher selenite-grafting extent than YPSe-I.

As shown in Table 2, nonylphenol at a dose of 120 μg/mL reduced viability value of IEC-6 cells to 65.7% (12 h) or 64.1% (24 h), while YP, YPSe-I, and YPSe-II were able to alleviate the nonylphenol-induced cytotoxicity in a dose-dependent manner. Specifically, YP, YPSe-I, and YPSe-II enhanced viability values to 65.7–74.5%, 66.8–78.4%, and 68.5–81.4% (12 h), or 67.2–77.4%, 69.5–79.3%, and 73.2–83.2% (24 h), respectively. An increase in

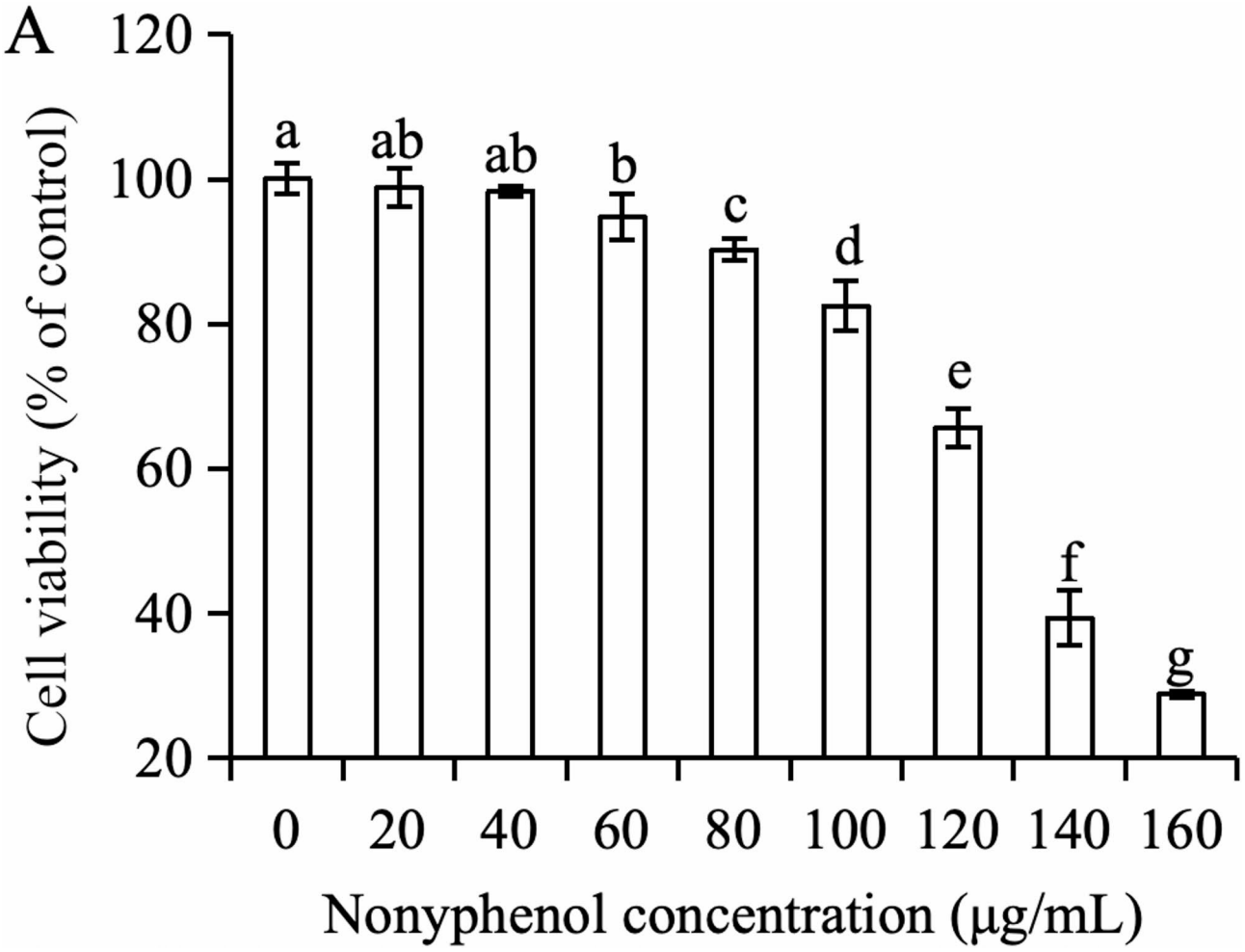

Fig. 1. Cytotoxicity of nonylphenol at eight doses to IEC-6 cells with a treatment time of 24 h. Different lowercase letters above the columns indicate that one-way ANOVA of the mean values differs significantly ($p < 0.05$).

Treatment time (h)	Sample	Cell viability (%) at different doses			
		5 μg/mL	10 μg/mL	20 μg/mL	40 μg/mL
12	YP	65.7 ± 2.7^{d}	66.0 ± 33.4^{d}	71.3 ± 2.0^{bc}	74.5 ± 1.7^{b}
	YPSe-I	66.8 ± 1.4^{d}	68.6 ± 2.3^{cd}	74.1 ± 3.1^{b}	78.4 ± 2.1^{a}
	YPSe-II	68.5 ± 1.2^{cd}	73.8 ± 1.9^{b}	79.1 ± 1.3^{a}	81.4 ± 1.6^{a}
	Nonylphenol	65.7 ± 2.1^{d} (at 120 μg/mL dose)			
24	YP	67.2 ± 1.5^{i}	70.7 ± 2.0^{gh}	74.1 ± 1.1^{ef}	77.4 ± 1.7^{cd}
	YPSe-I	69.5 ± 0.9^{hi}	72.6 ± 1.3^{fg}	76.4 ± 2.2^{de}	79.3 ± 0.8^{bc}
	YPSe-II	73.2 ± 1.1^{fg}	75.0 ± 1.4^{def}	80.7 ± 2.1^{ab}	83.2 ± 1.5^{a}
	Nonylphenol	64.1 ± 1.9^{j} (at 120 μg/mL dose)			

Table 2. Cell viability of the nonylphenol-induced IEC-6 cells with or without the exposure of Chinese Yam polysaccharides (YP) and selenite-grafted products YPSe-I and YPSe-II for 12 and 24 h. The control cells without nonylphenol and polysaccharide samples treatments were regarded with cell viability value of 100%. Different lowercase letters as the superscripts after the data with the same treatment time indicate that one-way ANOVA of the mean values differs significantly ($p < 0.05$).

viability value thus suggested decreased cytotoxicity of nonylphenol in the cells. A comparison of these data also indicated that YPSe-II had the highest activity but YP had the lowest activity in decreasing nonylphenol cytotoxicity. Hence, it was elucidated that both YP selenization and a higher selenite-grafting extent facilitated YPSe-I and YPSe-II to alleviate nonylphenol cytotoxicity in the cells.

Effect of polysaccharide samples on LDH release and ROS production in nonylphenol-induced cells

Generally, the extent of LDH release is an indicator of the extent of cell damage and barrier disruption. Our findings demonstrated that exposure to nonylphenol at a dose of 120 μg/mL elevated LDH release in IEC-6 cells, resulting in a relative LDH release exceeding 140%. In contrast, YP, YPSe-I, and YPSe-II at 5–40 μg/mL doses were capable of inhibiting LDH release in the nonylphenol-induced cells (Fig. 2A and B). When the cells were treated by YP, YPSe-I, and YPSe-II at the four doses for 12 h, the relative LDH release values decreased to 140.8–128.8%, 136.7–125.4%, and 131.3–118.3%, respectively. If the cells were treated with them for 24 h, the relative LDH release reduced to 135.3–119.6%, 133.0–117.4%, and 128.4–112.8%, respectively. Furthermore, this study also confirmed that nonylphenol could induce oxidative stress in the cells, leading to increased relative ROS production in the model cells (approximately 193%) (Fig. 2C and D). Meanwhile, YP, YPSe-I, and YPSe-II at the four doses suppressed ROS production in the nonylphenol-induced cells in a dose-dependent manner, reducing relative ROS production to 178–192%, 173–185%, and 167–180% (treatment time of 12 h), or 177–192%, 160–180%, and 153–172% (treatment time of 24 h), respectively. YP, YPSe-I, and YPSe-II were thus considered to possess two activities to counteract the nonylphenol-induced cell injury and oxidative stress in IEC-6 cells. These activities were achieved by reducing LDH release and inhibiting ROS formation.

Overall, the detected activities of the three polysaccharide samples followed an increasing order of YP < YPSe-I < YPSe-II. In other words, YP exhibited the weakest but YPSe-II had the strongest ability to alleviate the nonylphenol-induced cell injury and oxidative stress. The conducted covalent selenite-grafting of YP thus caused higher activity. It is hereinafter suggested that both YP selenization and a higher selenite-grafting extent were the contributing factors that enabled YPSe-I and YPSe-II to exert higher activities in the cells.

Effect of polysaccharides samples on TEER and paracellular permeability in nonylphenol-induced cells

To determine whether YP, YPSe-I, and YPSe-II could affect the permeability of the nonylphenol-injured cell monolayer, the TEER assay was conducted on IEC-6 cells (Fig. 3). IEC-6 cells exposed to 120 μg/mL nonylphenol only (i.e. the model cells) showed a reduced TEER than the control cells (relative value 70% *versus* 100%), indicating nonylphenol caused barrier loss or permeability increase. However, if the cells were also exposed to YP, YPSe-I, and YPSe-II at the four doses, they received an increase in TEER values. Specifically, when YP, YPSe-I, and YPSe-II were used to treat the cells for 12 h, the TEER values increased to 71.4–78.5%, 73.2–80.7%, and 74.2–85.3%, respectively; if these polysaccharide samples were used to incubate with the cells for 24 h, the TEER values enhanced to 72.3–81.3%, 78.3–87.5%, and 80.1–89.7%, respectively. Thus, YP, YPSe-I, and YPSe-II enhanced the barrier function of the nonylphenol-injured cell monolayer, and both YPSe-I and YPSe-II demonstrated higher activity than YP in enhancing cell barrier function.

The cells treated with YP, YPSe-I, and YPSe-II also had reduced paracellular permeability or improved barrier integrity (Fig. 3). Compared with the control cells (designated with 100% cumulative permeability of FD-4 or FS-Na), the model cells injured by 120 μg/mL nonylphenol showed barrier loss, evidenced by the increased paracellular permeability (137.2% for FD-4 and 148.3% for FS-Na). When the injured cells were exposed to YP, YPSe-I, and YPSe-II of the four doses for 12 h, the cumulative permeability of FD-4 (or FS-Na) decreased to 121.2–132.1%, 118.7–129.4%, and 116.3–127.4% (or 40.1–136.5%, 29.7–119.5%, and 22.3–95.6%), respectively. If the injured cells were treated with YP, YPSe-I, and YPSe-II of the four doses for 24 h, the measured cumulative permeability of FD-4 (or FS-Na) reduced to 118.2–130.3%, 114.6–127.2%, and 111.4–123.5% (or 34.7–130.4%, 25.5–110.2%, and 18.5–87.5%), respectively. Overall, higher dose of these polysaccharide samples led to much

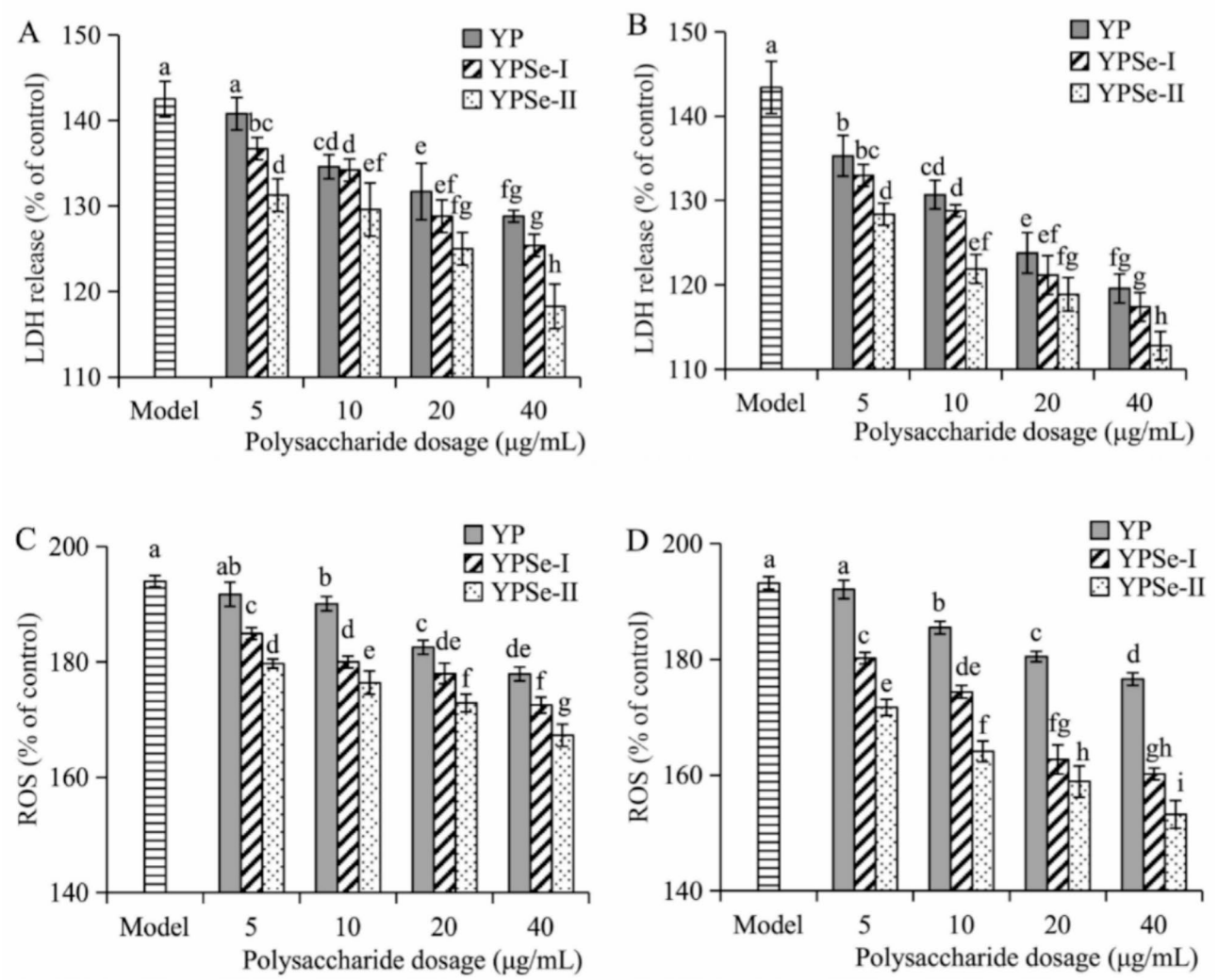

Fig. 2. LDH release (**A**, **B**) and relative ROS level (**C**, **D**) of nonylphenol-induced IEC-6 cells with or without the exposure of Chinese yam polysaccharides (YP) and selenite-grafted products YPSe-I and YPSe-II at the four doses for 12 (**A**, **C**) and 24 h (**B**, **D**). Different lowercase letters above the columns indicate that one-way ANOVA of the mean values differs significantly ($p < 0.05$).

decrease in cumulative permeability, while YP and YPSe-II showed the respective lowest and highest efficiency to reduce cumulative permeability.

The results presented in Fig. 3 proved that YP, YPSe-I, and YPSe-II in IEC-6 cells had the ability to counteract the nonylphenol-caused barrier loss. Considering their efficiency differences, it was concluded that both YP selenization and a higher selenite-grafting extent were two factors that endowed YPSe-I and YPSe-II with higher activity than YP in mitigating the nonylphenol-induced barrier damage. It is suggested that this selenization process might be a potential approach to enhance the beneficial function of native polysaccharides in the intestinal environment.

Effect of polysaccharide samples on F-actin distribution in nonylphenol-induced cells

To assess the impact of YP, YPSe-I, and YPSe-II on the distribution of critical F-actin in the nonylphenol-injured IEC-6 cells, the adherent cells were treated with 40 μg/mL polysaccharide samples for 12 and 24 h. The cells stained with Rhodamine-labeled phalloidin were thus observed under a fluorescence microscope to determine F-actin production and its distribution among the cells (Fig. 4).

The results confirmed that the control cells without any treatment were closely arranged while F-actin distribution among the cells was uniform. However, the model cells with 120 μg/mL nonylphenol exposure showed reduced fluorescence intensity of F-actin among the cells, suggesting that nonylphenol led to reduced F-actin production, poor F-actin distribution, and thereby impaired barrier integrity. When YP, YPSe-I, and YPSe-II were applied to the injured cells, the fluorescence signal intensity of F-actin was enhanced clearly, and the longer treatment duration with the polysaccharide samples led to stronger fluorescence signal intensity of F-actin. That meant that YP, YPSe-I, and YPSe-II could repair the injured cell barrier *via* promoting F-actin production and its proper distribution. The results also confirmed that YPSe-I especially YPSe-II were more

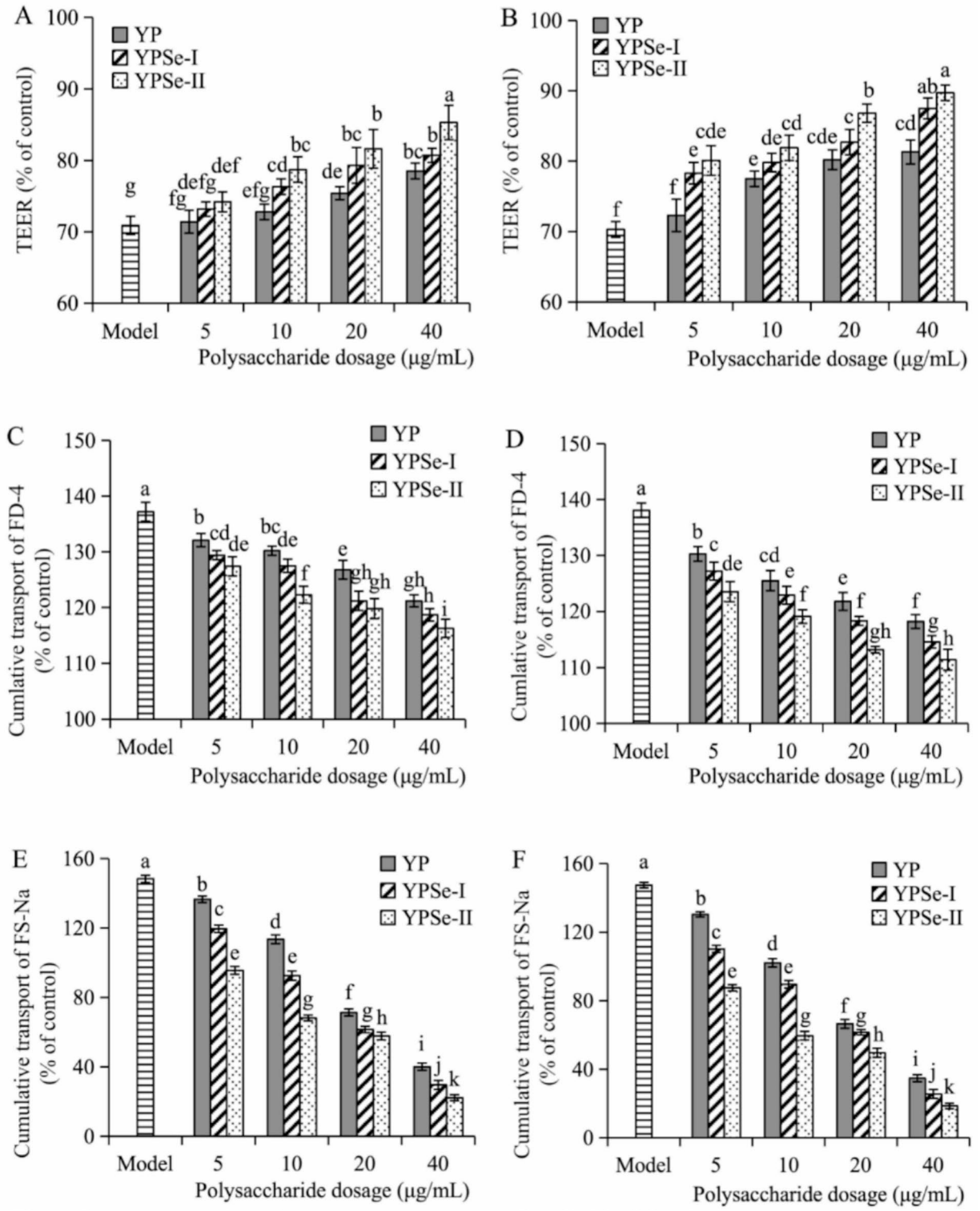

Fig. 3. Transepithelial electrical resistance (TEER) value (**A**, **B**), cumulative transport for FD-4 (**C**, **D**) and FS-Na (**E**, **F**) of nonylphenol-induced IEC-6 cells with or without the exposure of Chinese yam polysaccharides (YP) and selenite-grafted products YPSe-I and YPSe-II at the four doses for 12 (**A**, **C** & **E**) and 24 h (**B**, **D** & **F**). Different lowercase letters above the columns indicate that one-way ANOVA of the mean values differs significantly ($p < 0.05$).

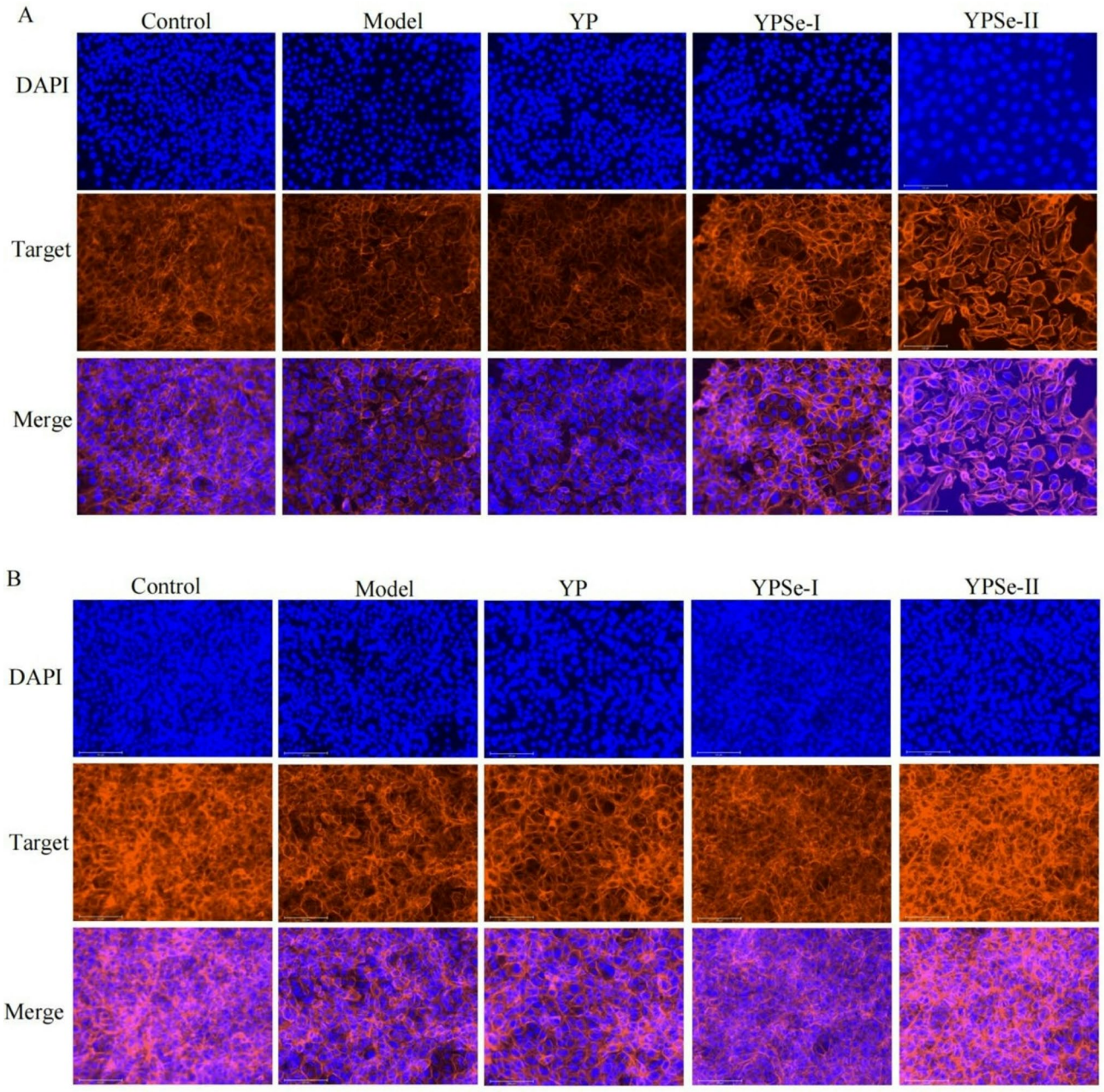

Fig. 4. F-actin distribution of nonylphenol-induced IEC-6 cells with or without the exposure of Chinese yam polysaccharides (YP) and selenite-grafted products YPSe-I and YPSe-II at 40 μg/mL for 12 (**A**) and 24 h (**B**). The scale of labeled bar is 125 μm.

active than YP in promoting F-actin production and distribution. In other words, both YP selenization and a higher selenite-grafting extent brought about higher activity for YPSe-I and YPSe-II in regulating F-actin production and distribution in IEC-6 cells.

Effect of polysaccharide samples on expression of TJ-related genes and proteins in nonylphenol-induced cells

To verify the barrier-protective effect of YP, YPSe-I, and YPSe-II in IEC-6 cells exposed to nonylphenol, both RT-qPCR and western-blot analyses were utilized to assess the expression of three TJ proteins including ZO-1, occludin, and claudin-1 at both mRNA and protein levels (Fig. 5), because the changes in barrier integrity was associated directly with the expression alteration of these TJ proteins.

The control cells were designed with relative mRNA or protein expression levels of 1.00 fold for ZO-1, occludin, and claudin-1. When the model cells were exposed to nonylphenol only for 24 h, relative mRNA expression levels of ZO-1, claudin-1, and occludin were down-regulated to 0.53, 0.42, and 0.53 fold, respectively. If the injured cells were also exposed to YP, YPSe-I, and YPSe-II, relative mRNA expression levels of ZO-1,

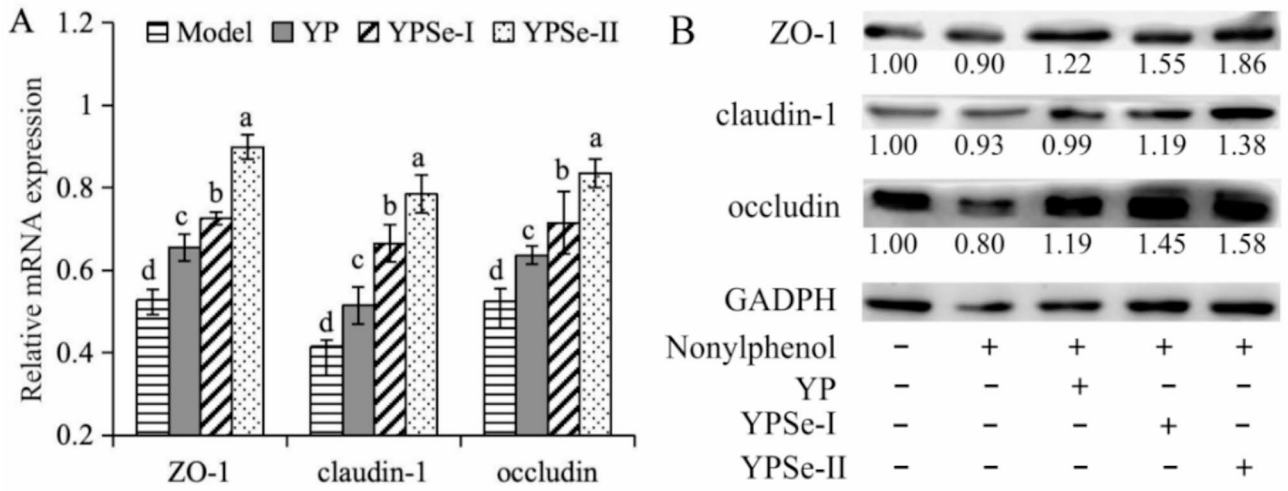

Fig. 5. Relative mRNA (**A**) and protein (**B**) expression of tight junction proteins ZO-1, claudin-1, and occludin in nonylphenol-induced IEC-6 cells with or without the exposure of Chinese yam polysaccharides (YP) and selenite-grafted products YPSe-I and YPSe-II at 40 μg/mL for 24 h. Different letters above the columns indicate that one-way ANOVA of the mean values differs significantly ($p < 0.05$).

claudin-1, and occludin were enhanced to 0.65–0.90, 0.51–0.78, and 0.64–0.83 fold, respectively. That is, YP, YPSe-I, and YPSe-II were capable of up-regulating the mRNA expression of the three TJ proteins. Meanwhile, although nonylphenol resulted in less protein expression for ZO-1, claudin-1, and occludin (0.80–0.93 fold) in the model cells, YP, YPSe-I, and YPSe-II could promote protein expression of the three TJ proteins (0.99–1.86 fold). These results consistently demonstrated that YP, YPSe-I, and YPSe-II could improve barrier function *via* up-regulating the expression of ZO-1, claudin-1, and occludin, while YP and YPSe-II had the respective lowest and highest activity in regulating TJ protein expression. It was regarded that both YP selenization and a higher selenite-grafting extent ensured YPSe-II with the highest activity in the cells to promote TJ protein expression and then repair the injured barrier function. More interestingly, the conclusion from both RT-qPCR and western-blot analyses were consistent with that from both TEER and paracellular permeability analyses.

Effect of polysaccharide samples on MAPK signaling pathway

It is known that cellular oxidative stress of cells is associated with the MAPK signaling pathway. It was also verified in a previous study that 6-gingerol could regulate cell barrier function *via* this signaling pathway[27] Based on the fact that nonylphenol induced excessive ROS production in IEC-6 cells, it was necessary to determine whether this pathway was involved in the barrier protection of these polysaccharide samples in IEC-6 cells.

Two proteins namely p-JNK and p-p38, which are critical to the activation of the MAPK signaling pathway, were thus evaluated briefly for their expression alteration at both mRNA and protein levels in the cells (Fig. 6). Compared with the control cells, the model cells exposed to nonylphenol alone exhibited an up-regulated relative mRNA expression for p-JNK (1.27 fold) and p-p38 (1.35 fold). Upon exposing to YP, YPSe-I, and YPSe-II for 24 h, the cells showed a reduction in relative mRNA expression for p-JNK (0.85–1.17 fold) and p-p38 (0.99–1.21 fold), compared with the model cells. Simultaneously, the model cells were detected with up-regulated relative protein expression for p-JNK (1.13 fold) and p-p38 (1.19 fold), while the three polysaccharide samples decreased relative protein expression of p-JNK and p-p38 to 0.41–0.90 and 0.54–0.72 fold, respectively. Clearly, nonylphenol induced the activation of the MAPK signaling pathway, while YP, YPSe-I, and YPSe-II demonstrated the ability to suppress this activation. Moreover, YPSe-I especially YPSe-II had a higher potent than YP to suppress this activation. It was thus proposed that YPSe-I especially YPSe-II could protect barrier function of the induced cells partly through an inactivation on this MAPK signaling pathway.

Discussion

When nonylphenol enters into environment and subsequently the food chain, various foods including drinking water are exposed to nonylphenol pollution. When the body ingests the nonylphenol-polluted foods, the gastrointestinal tract becomes the first tissue that is exposed to nonylphenol toxicity. Intestinal epithelial cells play a crucial role as the first physical defense line against external harmful substances including nonylphenol. Hence, after the body ingests these nonylphenol-contaminated foods, intestinal epithelial cells might become a potential target for the nonylphenol-induced toxicity, leading to intestinal damage. Previous results revealed that nonylphenol had clear cytotoxic effect on ASK cells[31] Meanwhile, it was reported that when 40 μmol/L nonylphenol was applied on Caco-2 cells for 48 h, the intracellular contents of ROS and malondialdehyde were increased, while LDH release was also elevated, indicating nonylphenol's toxicity on Caco-2 cells[32] In addition, certain active substances in foods can alleviate the damage of certain foreign substances to the intestinal barrier. For example, the polysaccharides isolated from *Hericium erinaceus* could effectively improve the intestinal barrier function of Muscovy ducklings infected with Muscovy duck reovirus,[33] while paeoniflorin was capable of

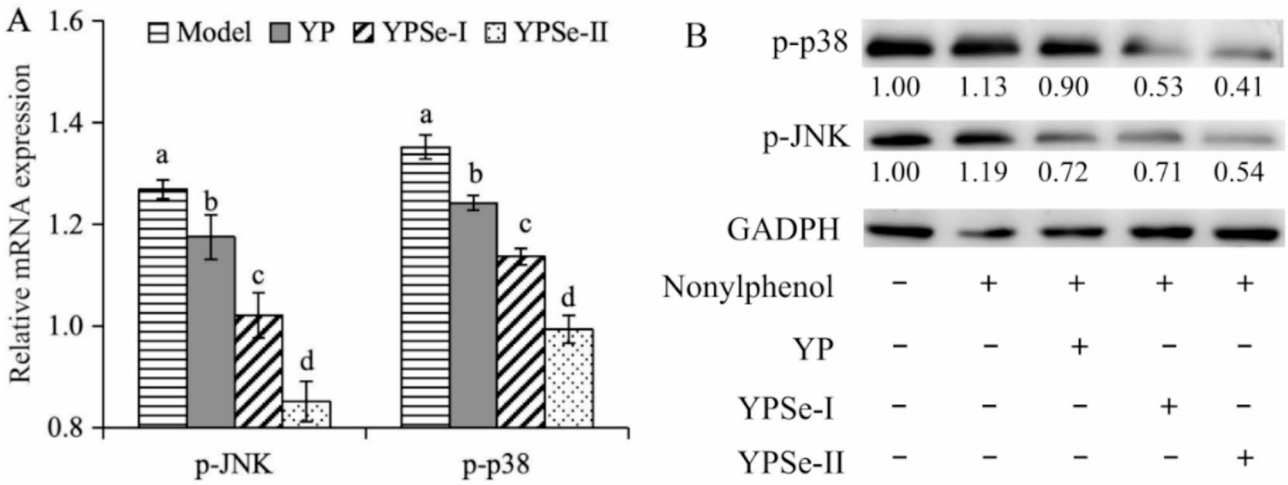

Fig. 6. Relative mRNA (**A**) and protein (**B**) expression of p-JNK and p-p38 in nonylphenol-induced IEC-6 cells with or without the exposure of Chinese yam polysaccharides (YP) and selenite-grafted products YPSe-I and YPSe-II at 40 μg/mL for 24 h. Different letters above the columns indicate that one-way ANOVA of the mean values differs significantly ($p < 0.05$).

ameliorating the lipopolysaccharide-induced barrier loss in Caco−2 cells[34] Moreover, two polyphenols galangin and kaempferol were reported to alleviate the indomethacin-induced barrier damage in IEC−6 cells[12] In line with the conclusion of these reported studies, the present study declared that both YPSe-I and YPSe-II possessed ability to alleviate the nonylphenol-induced adverse effect in IEC-6 cells, resulting in higher cell viability, reduced LDH release and ROS production, and improved barrier integrity.

Generally, TEER and paracellular permeability are two useful indicators that reflect the integrity of cell barrier. When harmful factors cause damage on intestinal barrier, TEER value will be decreased while paracellular permeability thereby is enhanced. When cell barrier function is enhanced or repaired by certain agents, TEER value will be increased but the paracellular permeability is suppressed. It was observed that the *Alpinia officinarum* Hance polysaccharie could promote the growth of Caco-2 cells and improve their barrier function by increasing TEER value,[35] while glycated casein digest could increase TEER value of the acrylamide-exposed IEC-6 cells and reduce the cumulative permeation of FD-4[11] Similarly, the present study also found that these polysaccharide samples caused an increase in TEER but a decrease in paracellular permeability in the injured IEC-6 cells. Moreover, TJ proteins and F-actin can collaborate to maintain cell barrier function[36] Barrier function constituted by TJ proteins thus regulates paracellular permeability between cells, while F-actin ensures the effective implementation of this barrier function through its supportive and stabilizing action on TJ proteins[37] In the presence of inflammation or stress, F-actin can modulate the state of TJ proteins through its own dynamic reorganization to continuously maintain barrier function between cells[38] It was revealed that when MDCK cells were treated with 100 μg/mL calcium oxalate for 48 h, the expression of F-actin between the cells was inhibited; simultaneously, the expression of ZO-1 was also decreased[39] When HOCl or H_2O_2 were used to injure Caco−2 cells, F-actin distribution between cells decreased[40] Regarding these important food pollutants and toxins such as acrylamide, indomethacin, fumonisin B1, nonylphenol, and others, it had been verified in the previous studies that they might cause barrier dysfunction *via* reducing the production of TJ proteins[11123035] However, several food components have been identified to up-regulate TJ protein expression, resulting in the restoration of cell barrier function[11123035] In the present study, although nonylphenol damaged barrier function of IEC-6 cells *via* suppressing F-actin production and distribution and reducing TJ protein production, IEC-6 cells treated with YP especially YPSe-I and YPSe-II were resistant to the nonylphenol-induced barrier injury, and thus showed the improved F-actin production and distribution, together with the up-regulated TJ protein production. The present study thus shared conclusion consistence with these mentioned studies.

Generally, chemical modification like sulfonation, phosphorylation, acetylation, and selenization can enhance the bioactivity of natural polysaccharides. For instance, Peng and coauthors found that Citrus polysaccharides after sulfonation possessed higher activity in scavenging DPPH and ABTS radicals, and also showed higher immunomodulatory ability[41] Zhang and coauthors revealed that phosphorylated *Trichosanthes kirilowii* polysaccharides had enhanced antiaging activity in the mouse model,[42] while Tang and coauthors stated that the Luohan fruit peel polysaccharides after acetylation had better antioxidant capacity[43] A previous study of our research group indicated that the selenylated longan polysaccharides could rescue fumonisin B1-damaged intestinal barrier function through the MAPK and mitochondrial apoptosis pathways, while a higher selenylation extent could further enhance polysaccharide activity[30] The sulfated *Gracilaria lemaneiformis* polysaccharides could also promote the expression of TJ proteins and mucin 2, thereby enhancing intestinal barrier in colitis mice[44] Additionally, the selenylated *Ulva pertusa* polysaccharides could effectively enhance intestinal barrier function in the mice with inflammatory bowel disease (IBD)[45] The present study thereby highlighted that chemical selenization of natural polysaccharides could lead to higher activity in protecting intestinal barrier. This activity increase meant that the selenized polysaccharides had higher potential as

bioactive materials for the IBD patients, considering that a symptomatic care for the IBD patients is urgent in both food and medicine fields. Furthermore, the present study found another interesting fact; that is, a higher selenite-grafting of YP led to increased activity for YPSe-I and YPSe-II in the cells. It was thereby proposed that both chemical selenization and a higher selenite-grafting extent were two factors controlling the bioactivity of YPSe-I and YPSe-II. Similarly, our previous studies also observed that the two factors controlled the activities of selenized logan polysaccharides and selenized purslane polysaccharides[234647].

The regulation of the so-called MAPK signaling pathway is considered to be related to cellular oxidative stress and associated with pathological mechanisms such as inflammation in intestinal damage[48] The main family members of the MAPK signaling pathway include JNK, ERK, and p38. The phosphorylation of these proteins can trigger the activation of this signaling pathway[49] When cells are stimulated by external conditions like inflammatory cytokines and oxidative stress, JNK, ERK, and p38 can be activated and then participate in the regulation of this signaling pathway in the phosphorylated forms[50] Food components in cells can improve cell barrier function *via* this signaling pathway. For example, a flavonoid compound resveratrol could regulate the MAPK signaling pathway by acting on relevant receptors[51] In a cyclophosphamide-injured mouse model, the resulted intestinal barrier damage could be ameliorated by *Cordyceps sinensis* polysaccharides *via* inactivating the MAPK signaling pathway[52] Another example was the study from Peng and coauthors, in which lentil hulls procyanidin could enhance barrier function of Caco-2 cells through the MAPK signaling pathway[53] The present study found nonylphenol's ability to up-regulate the expression of both p-JNK and p-p38, and then triggered the activation of the MAPK pathway pathway. Meanwhile, YP, especially YPSe-I and YPSe-II, were capable of down-regulate the expression of p-JNK and p-p38, and thereby resulting in the inactivation of this pathway pathway. It was thus concluded that these samples could alleviate or rescue the nonylphenol-induced barrier loss in IEC-6 cells *via* suppressing the activation of the MAPK signaling pathway.

Although it had been verified in the present study that the selenite-grafted YP products could alleviate the nonylphenol-induced barrier damage in IEC-6 cells through the MAPK signaling pathway, previous studies had indicated that other signaling pathways such as NF-κB, ROCK/RhoA, and PI3K/Akt signaling pathways might be involved in the studied models.53[55] Thus, our future research might focus specifically on these signaling pathways. Moreover, other activities (e.g. anti-inflammatory effect and regulation on gut microbiota) of the selenized polysaccharides need an in vitro and especially in vivo investigation.

Conclusion

When natural YP were subjected to the aforementioned covalent selenization, the selenite-grafted YP products had higher Se contents and in particular higher activities in intestinal epithelial IEC-6 cells with nonylphenol exposure. These increased activities enabled them to alleviate the nonylphenol-induced cell toxicity and barrier dysfunction in IEC-6 cells, resulting higher cell viability, reduced LDH release, decreased ROS production, increased TEER value, reduced paracellular permeability, and increased production of cytoskeleton F-actin and three TJ proteins namely ZO-1, occludin, and claudin-1. It was also verified that the selenite-grafted YP products inhibited the nonylphenol-induced activation of the MAPK signaling pathway and subsequently possessed the ability to repair barrier loss. Furthermore, both YP selenization and a higher selenite-grafting extent were determined to be two factors that contributing to the enhanced activities of YPSe-I and YPSe-II. It is also proposed here that this chemical selenization is an effective approach to improve the healthy function of natural polysaccharides in the intestine environment, considering the possible adverse effects of these pollutants in the intestine to cause cell toxicity and barrier damage.

Data availability

Data is provided within the manuscript.

Received: 9 December 2024; Accepted: 19 May 2025
Published online: 23 May 2025

References

1. De La Fuente, L. et al. Degradation of nonylphenol ethoxylate-9 (NPE-9) by photochemical advanced oxidation technologies. *Ind. Eng. Chem. Res.* **49**, 6909–6915. https://doi.org/10.1021/ie901785j (2010).
2. Gałązka, A. & Jankiewicz, U. Endocrine disrupting compounds (nonylphenol and bisphenol A)—sources, harmfulness and laccase-assisted degradation in the aquatic environment. *Microorganisms* **10**, e2236. https://doi.org/10.3390/microorganisms10112236 (2022).
3. Miao, B. et al. A review on Human biomonitoring, toxicity, detection and treatment in the environment. *Molecules* **28**, e2505. (2023). https://doi.org/10.3390/molecules28062505
4. Lu, J., Wu, J., Stoffella, P. J. & Wilson, P. C. Uptake and distribution of bisphenol A and nonylphenol in vegetable crops irrigated with reclaimed water. *J. Hazard. Materi.* **283**, 865–870. https://doi.org/10.1016/j.jhazmat.2014.10.018 (2015).
5. Careghini, A., Mastorgio, A. F., Saponaro, S., Sezenna, E. & Bisphenol A, nonylphenols, benzophenones, and benzotriazoles in soils, groundwater, surface water, sediments, and food: A review. *Environ. Sci. Pollut Res.* **22**, 5711–5741. https://doi.org/10.1007/s11356-014-3974-5 (2015).
6. Bhandari, G., Bagheri, A. R., Bhatt, P. & Bilal, M. Occurrence, potential ecological risks, and degradation of endocrine disrupter, nonylphenol, from the aqueous environment. *Chemosphere* **275**, e130013. https://doi.org/10.1016/j.chemosphere.2021.130013 (2021).
7. Noorimotlagh, Z. et al. Environmental exposure to nonylphenol and cancer progression Risk–A systematic review. *Environ. Res.* **184**, e109263. https://doi.org/10.1016/j.envres.2020.109263 (2020).
8. Vancamelbeke, M. & Vermeire, S. The intestinal barrier: A fundamental role in health and disease. *Expert Rev. Gastroenterol. Hepatol.* **11**, 821–834. https://doi.org/10.1080/17474124.2017.1343143 (2017).
9. Huo, J. Y. et al. Protective effects of natural polysaccharides on intestinal barrier injury: A review. *J. Agric. Food Chem.* **70**, 711–735. https://doi.org/10.1021/acs.jafc.1c05966 (2022).

10. Suzuki, T. Regulation of the intestinal barrier by nutrients: The role of tight junctions. *Anim. Sci. J.* **91**, e13357. https://doi.org/10.1111/asj.13357 (2020).
11. Shi, J. & Zhao, X. H. Chemical features of the oligochitosan-glycated caseinate digest and its enhanced protection on barrier function of the acrylamide-injured IEC-6 cells. *Food Chem.* **290**, 246–254. https://doi.org/10.1016/j.foodchem.2019.04.004 (2019).
12. Fan, J., Zhao, X. H., Zhao, J. R. & Li, B. R. Galangin and Kaempferol alleviate the indomethacin-caused cytotoxicity and barrier loss in rat intestinal epithelial (IEC-6) cells *via* mediating JNK/Src activation. *ACS Omega*. **6**, 15046–15056. https://doi.org/10.1021/acsomega.1c01167 (2021).
13. Lu, S. Y. et al. Gracilaria lemaneiformis polysaccharides alleviate colitis by modulating the gut microbiota and intestinal barrier in mice. *Food Chem. X*. **13**, e100197. https://doi.org/10.1016/j.fochx.2021.100197 (2022).
14. Górska, S., Maksymiuk, A. & Turło, J. Selenium-containing polysaccharides–structural diversity, biosynthesis, chemical modifications and biological activity. *Appl. Sci.* **11**, e3717. https://doi.org/10.3390/app11083717 (2021).
15. Li, C. P. et al. Selenization of ovalbumin by dry-heating in the presence of selenite: Effect on protein structure and antioxidant activity. *Food Chem.* **148**, 209–217. https://doi.org/10.1016/j.foodchem.2013.10.033 (2014).
16. Kieliszek, M. et al. Metabolic ˙response of the yeast Candida utilis during enrichment in selenium. *Int. J. Mol. Sci.* **21**, e5287. https://doi.org/10.3390/ijms21155287 (2020).
17. Fang, Y. et al. Isolation and identification of Immunomodulatory selenium-containing peptides from selenium-enriched rice protein hydrolysates. *Food Chem.* **275**, 696–702. https://doi.org/10.1016/j.foodchem.2018.09.115 (2019).
18. Yuan, M. H. et al. Selenized modification and structural characterization of *Pleurotus eryngii* polysaccharides and their Immunomodulatory activity. *Process. Biochem.* **144**, 97–111. https://doi.org/10.1016/j.procbio.2024.05.018 (2024).
19. Feng, X. J. et al. The structural characterization of a novel Chinese Yam polysaccharide and its hypolipidemic activity in HFD-induced obese C57BL/6J mice. *Int. J. Biol. Macromol.* **265**, e130521. https://doi.org/10.1016/j.ijbiomac.2024.130521 (2024).
20. Bai, Y. J. et al. Gut microbial fermentation promotes the intestinal anti-inflammatory activity of Chinese Yam polysaccharides. *Food Chem.* **402**, e134003. https://doi.org/10.1016/j.foodchem.2022.134003 (2023).
21. Hao, L. X. & Zhao, X. H. Immunomodulatory potentials of the water-soluble Yam (*Dioscorea opposita* Thunb) polysaccharides for the normal and cyclophosphamide-suppressed mice. *Food Agric. Immunol.* **27**, 667–677. https://doi.org/10.1080/09540105.2016.1148666 (2016).
22. Surhio, M. M. et al. Antihyperlipidemic and hepatoprotective properties of selenium modified polysaccharide from *Lachnum* Sp. *Int. J. Biol. Macromol.* **99**, 88–95. https://doi.org/10.1016/j.ijbiomac.2017.01.148 (2017).
23. Yu, Y. H., Wang, L., Zhang, Q., Zhang, X. N. & Zhao, X. H. Activities of the soluble and non-digestible Longan (*Dimocarpus Longan Lour.*) polysaccharides against HCT-116 cells as affected by a chemical selenylation. *Curr. Res. Food Sci.* **5**, 1071–1083. https://doi.org/10.1016/j.crfs.2022.06.008 (2022).
24. Sebaugh, J. L. Guidelines for accurate EC50/IC50 estimation. *Pharm. Stat.* **10**, 128–134. https://doi.org/10.1002/pst.426 (2011).
25. Li, F. F. et al. Polysaccharide from the seeds of *Plantago asiatica* L. alleviates nonylphenol induced intestinal barrier injury by regulating tight junctions in human Caco-2 cell line. *Int. J. Biol. Macromol.* **164**, 2134–2140. https://doi.org/10.1016/j.ijbiomac.2020.07.259 (2020).
26. Canali, M. M., Pedrotti, L. P., Balsinde, J., Ibarra, G. & Correa, S. G. Chitosan enhances transcellular permeability in human and rat intestine epithelium. *Eur. J. Pharm. Biopharm.* **80**, 418–425. https://doi.org/10.1016/j.ejpb.2011.11.007 (2012).
27. Li, Y. L. et al. 6-Gingerol protects intestinal barrier from ischemia/reperfusion-induced damage *via* Inhibition of p38 MAPK to NF-κB signalling. *Pharmacol. Res.* **119**, 137–148. https://doi.org/10.1016/j.phrs.2017.01.026 (2017).
28. Bouley, R., Yui, N., Terlouw, A., Cheung, P. W. & Brown, D. Chlorpromazine induces basolateral aquaporin-2 accumulation via F-actin depolymerization and Blockade of endocytosis in renal epithelial cells. *Cell* **9**, e1057. https://doi.org/10.3390/cells9041057 (2020).
29. Wang, Z. X. & Zhao, X. H. The barrier-enhancing function of soluble Yam (*Dioscorea opposita* Thunb.) polysaccharides in rat intestinal epithelial cells as affected by the covalent se conjugation. *Nutrients* **14**, e3950. https://doi.org/10.3390/nu14193950 (2022).
30. Yu, Y. H. & Zhao, X. H. Longan polysaccharides with covalent selenylation combat the Fumonisin B1-induced cell toxicity and barrier disruption in intestinal epithelial (IEC-6) cells. *Nutrients* **15**, e4679. https://doi.org/10.3390/nu15214679 (2023).
31. Salazar, C., Ojeda, N. & Mercado, L. Dysregulated Proinflammatory cytokines and immune-related MiRNAs in ASK cells exposed to 17α-Ethynyl estradiol and 4-nonylphenol. *Dev. Comp. Immunol.* **162**, e105282. https://doi.org/10.1016/j.dci.2024.105282 (2025).
32. Ding, F. F. et al. Polystyrene microplastics with absorbed nonylphenol induce intestinal dysfunction in human Caco-2 cells. *Environ. Toxicol. Pharmacol.* **107**, e104426. https://doi.org/10.1016/j.etap.2024.104426 (2024).
33. Wu, Y. J. et al. *Hericium erinaceus* polysaccharide facilitates restoration of injured intestinal mucosal immunity in muscovy Duck reovirus-infected muscovy Ducklings. *Int. J. Biol. Macromol.* **107**, 1151–1161. https://doi.org/10.1016/j.ijbiomac.2017.09.092 (2008).
34. Wu, X. X. et al. Paeoniflorin prevents intestinal barrier disruption and inhibits lipopolysaccharide (LPS)-induced inflammation in Caco-2 cell monolayers. *Inflammation* **42**, 2215–2225. https://doi.org/10.1007/s10753-019-01085-z (2019).
35. Jia, X. J. et al. The use of polysaccharide AOP30 from the rhizome of *Alpinia officinarum* hance to alleviate lipopolysaccharide-induced intestinal epithelial barrier dysfunction and inflammation via the TLR4/NfκB signaling pathway in Caco-2 cell monolayers. *Nutrients* **16**, e2151. https://doi.org/10.3390/nu16132151 (2024).
36. Shen, L. Tight junctions on the move: Molecular mechanisms for epithelial barrier regulation. *Ann. N. Y. Acad. Sci.* **1258**, 9–18. https://doi.org/10.1111/j.1749-6632.2012.06613.x (2012).
37. Moonwiriyakit, A. et al. Tight junctions: From molecules to Gastrointestinal diseases. *Tissue Barriers*. **11**, e2077620. https://doi.org/10.1080/21688370.2022.2077620 (2023).
38. Marcos-Ramiro, B., García-Weber, D. & Millán, J. TNF-induced endothelial barrier disruption: Beyond actin and Rho. *Thromb. Haemostasis*. **112**, 1088–1102. https://doi.org/10.1160/th14-04-0299 (2014).
39. Peerapen, P. & Thongboonkerd, V. Calcium oxalate monohydrate crystal disrupts tight junction via F-actin reorganization. *Chem. Biol. Interact.* **345**, e109557. https://doi.org/10.1016/j.cbi.2021.109557 (2021).
40. Banan, A., Fitzpatrick, L., Zhang, Y. & Keshavarzian, A. OPC-compounds prevent oxidant-induced carbonylation and depolymerization of the F-actin cytoskeleton and intestinal barrier hyperpermeability. *Free Radical Biol. Med.* **30**, 287–298. https://doi.org/10.1016/s0891-5849(00)00471-8 (2001).
41. Peng, B. et al. Isolation, structural characterization, and immunostimulatory activity of a new water-soluble polysaccharide and its sulfated derivative from *Citrus medica* L. Var. Sarcodactylis. *Int. J. Biol. Macromol.* **123**, 500–511. https://doi.org/10.1016/j.ijbiomac.2018.11.113 (2019).
42. Zhang, M. et al. Phosphorylation and antiaging activity of polysaccharide from Trichosanthes Peel. *J. Food Drug Anal.* **25**, 976–983. https://doi.org/10.1016/j.jfda.2016.12.013 (2017).
43. Tang, Z. J., Huang, G. L. & Huang, H. L. Ultrasonic-assisted extraction, analysis and properties of purple mangosteen Scarfskin polysaccharide and its acetylated derivative. *Ultrason. Sonochem.* **109**, e107010. https://doi.org/10.1016/j.ultsonch.2024.107010 (2024).
44. Han, R. et al. The possible mechanism of the protective effect of a sulfated polysaccharide from Gracilaria Lemaneiformis against colitis induced by dextran sulfate sodium in mice. *Food Chem. Toxicol.* **149**, e112001. https://doi.org/10.1016/j.fct.2021.112001 (2021).

45. Wang, Y. et al. Intestinal anti-inflammatory effects of selenized *Ulva pertusa* polysaccharides in a dextran sulfate sodium-induced inflammatory bowel disease model. *J. Med. Food.* **24**, 236–247. https://doi.org/10.1089/jmf.2020.4787 (2021).
46. Li, L. Y. et al. Monosaccharide composition and *in vitro* activity to HCT-116 cells of purslane polysaccharides after a covalent chemical selenylation. *Foods* **11**, e3748. https://doi.org/10.3390/foods11233748 (2022).
47. Lin, Y. R. et al. In vitro immuno-modulatory potentials of purslane (*Portulaca oleracea* L.) polysaccharides with a chemical selenylation. *Foods* **11** (e14). https://doi.org/10.3390/foods11010014 (2022).
48. Vona, R., Pallotta, L., Cappelletti, M., Severi, C. & Matarrese, P. The impact of oxidative stress in human pathology: Focus on Gastrointestinal disorders. *Antioxidants* **10**, e201. https://doi.org/10.3390/antiox10020201 (2021).
49. Barr, R. K. & Bogoyevitch, M. A. The c-Jun N-terminal protein kinase family of mitogen-activated protein kinases (JNK MAPKs). *Int. J. Biochem. Cell. Biol.* **33**, 1047–1063. https://doi.org/10.1016/S1357-2725(01)00093-0 (2001).
50. Son, Y., Kim, S., Chung, H. T. & Pae, H. O. Reactive oxygen species in the activation of MAP kinases. *Methods Enzymol.* **528**, 27–48. https://doi.org/10.1016/B978-0-12-405881-1.00002-1 (2013).
51. Jo, H., Hwang, D., Kim, J. K. & Lim, Y. H. Oxyresveratrol improves tight junction integrity through the PKC and MAPK signaling pathways in Caco-2 cells. *Food Chem. Toxicol.* **108**, 203–213. https://doi.org/10.1016/j.fct.2017.08.002 (2017).
52. Ying, M. X. et al. Cultured cordyceps sinensis polysaccharides attenuate cyclophosphamide-induced intestinal barrier injury in mice. *J. Funct. Foods.* **62**, e103523. https://doi.org/10.1016/j.jff.2019.103523 (2019).
53. Peng, L. et al. Anti-inflammatory effect of lentil hull (*Lens culinaris*) extract via MAPK/NF-κB signaling pathways and effects of digestive products on intestinal barrier and inflammation in Caco-2 and Raw264.7 co-culture. *J. Funct. Foods.* **92**, e105044. https://doi.org/10.1016/j.jff.2022.105044 (2022).
54. Zhao, D. Y., Jiao, S. W. & Yi, H. L. Arsenic exposure induces small intestinal toxicity in mice by barrier damage and inflammation response via activating RhoA/ROCK and TLR4/Myd88/NF-κB signaling pathways. *Toxicol. Lett.* **384**, 44–51. https://doi.org/10.1016/j.toxlet.2023.07.007 (2023).
55. Liu, J. et al. *Bacillus subtilis* and xylo-oligosaccharide ameliorates $NaHCO_3$-induced intestinal barrier dysfunction and autophagy by regulating intestinal microflora and PI3K/Akt pathway of crucian carp (*Carassius auratus*). *Aquacult. Rep.* **36**, e102048. https://doi.org/10.1016/j.aqrep.2024.102048 (2024).

Acknowledgements

This research was funded by the Scientific Research Foundation of Guangdong University of Petrochemical Technology (Project No. 2020rc026).

Author contributions

Zhen-Xing Wang: Formal analysis, Investigation, Methodology, & Writing - Original Draft. Li-Li Zhang: Formal analysis, Methodology, Supervision. Xin-Huai Zhao: Conceptualization, Supervision, Project administration, Funding acquisition & Writing - Review & Editing.

Declarations

Competing interests

The authors declare no competing interests.

Additional information

Correspondence and requests for materials should be addressed to X.-H.Z.

Reprints and permissions information is available at www.nature.com/reprints.

Publisher's note Springer Nature remains neutral with regard to jurisdictional claims in published maps and institutional affiliations.